Bandgap Broadening in a Membrane Acoustic Metamaterial with Multiple Resonators and Membrane Layers

Aidin Nojavan, Sabine C. Langer[2]

[1] *Institut für Konstruktionstechnik, 38106 Braunschweig, E-Mail:a.nojavan@tu-braunschweig.de*
[2] *Institut für Konstruktionstechnik, 38106 Braunschweig, E-Mail: s.langer@tu-braunschweig.de*

Abstract

Locally resonant acoustic metamaterials (LRAM) are known as an innovative solution to acoustic insulation, which possess a high efficiency in sound attenuation besides compactness and low weight. However, they present their outstanding functionality at a narrow frequency range, known as bandgap. This tightly limited operation range of LRAMs is considered as their most important disadvantage. In this study, the performance of a membrane type acoustic metamaterial in presence of a concentrated force is examined numerically by calculating its velocity level using Finite Element Method (FEM). Also, its bandgap is attempted to be extended by manipulating local resonances within the LRAM by using multiple resonators and membranes.

Keywords: acoustic metamaterial, membrane, bandgap

Introduction

Locally Resonant Acoustic Metamaterial (LRAM) refers to a category of engineered materials, which provide a great degree of wave attenuation with the help of local resonances within their structure. This is possible by modifying the structure of the material in micro scale. The approach is generally to utilize micro-structured resonators, which are isolated with a layer of a soft elastic material from the main structure or crystal. This provides extra degrees of freedom for the structure. At the local resonance frequency, namely the resonance frequency of the resonator, a phase delay of π takes place between the resonator acceleration within the elastic medium and the applied force, meaning that the resonator brings a restoring force, opposite to the external applied force. Using this principle, LRAMs are able to provide extraordinary characteristics, not seen normally in the nature [1]. The resonance frequency depends on the inertia (mass) of the resonant and the restoring force. Hence, the relevant wavelength can be orders of magnitude larger than the geometry of the unit cell [2,3].

Liu et al. [4] are among the first, examining LRAM characteristics. They calculated amplitude transmission coefficient in a LRAM crystal, containing 8×8×8 core-coated unit cells, and also measured it experimentally. Their “sonic crystal” showed an almost complete band gap [4, 3]. In 2008, Yang et al. introduced the membrane type LRAM, which is principally similar to the core-coat type, but thinner in one dimension. In a membrane acoustic metamaterial (MAMM), which is shown schematically in Fig. 1, a solid frame holds a layer of an elastic membrane within itself, on which, a relatively dense disk is mounted to serve as a resonator. Yang et al. [5] indicated the possibility of sound insulation within a narrow-band using a mass-membrane AMM. It was later shown in another study [6] that by using multiple weights per cell plus stacking several membrane panels operative in different frequency regimes, a broad frequency effectiveness can be achieved. In a more recent study, Fan et al. [7] coated both surfaces of periodically perforated plates by membranes in aim for low-frequency sound insulation. Wang et al. \cite{WZHL16} characterized a membrane-constrained acoustic metamaterial, which is realized by using sticks to constrain the motions of the membrane in the near-total transmission modes at low frequencies. Their "membrane-constrained" acoustic metamaterial showed the broadest bandwidth compared with two similar conventional ones.

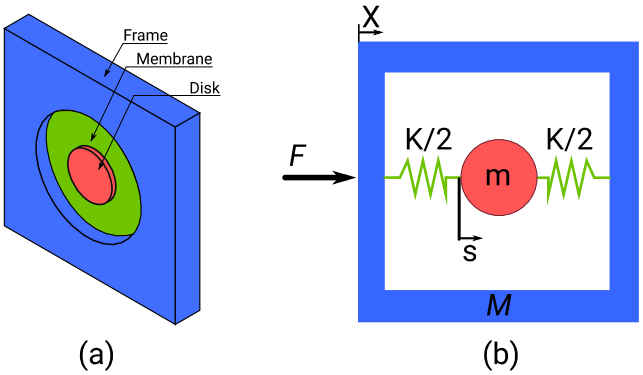

Fig 1– (a) Schematic view of a typical MAMM unit cell (b) Mass-spring model representing a MAMM

In this study, the performance of a membrane type acoustic metamaterial in presence of a concentrated force is examined numerically by calculating its velocity level using Finite Element Method (FEM). Also, its bandgap is attempted to be extended by manipulating local resonances within the LRAM by using multiple resonators and membranes.

Physics of Membrane Acoustic Metamaterials

The physics behind the MAMM is based on extra hidden degrees of freedom within its structure. A mass-spring model of a MAMM unit cell (UC) is shown schematically in **Fig. 1**, in which the damping effects of materials are neglected. In the figure, mass M stands for the frame of MAMM, whereas mass m refers to the resonant disk. The elastic membrane is modeled as a spring, where its mass is neglected and the focus is on its elastic characteristics.

If a harmonic force F is applied to the frame in a frictionless field, and the replacement of the frame and the resonator are stated respectively with X and s, the following system of equations can describe the motions of the involved components for the case, where $s > X$:

$$F + K\,(s - X) = M\,\ddot{X} \qquad (3)$$

$$-K\,(s\,-X) = m\,\ddot{s} \tag{4}$$

Where K refers to the spring constant. Combining these two equations of motion gives the general equation for the whole system as in equation (5):

$$F = M\,\ddot{X} + m\ddot{s} \tag{5}$$

The harmonic displacement for a mass-spring system can be generally formulated as in what follows:

$$x(\omega t) = \hat{x}e^{j\omega t} \tag{6}$$

If we suppose that ω and ω_0 are the resonance frequencies of the frame M and the resonator m, the local resonance frequency of the core, then the following equation can be concluded from equation (4) for an excitation at frequency ω:

$$-\omega^2 s = -\omega_0^2\,(s - X) \tag{7}$$

Where the local resonance frequency ω_0 can be calculated with equation (8):

$$\omega_0 = \sqrt{K/m} \tag{8}$$

Considering the term of acceleration in equation (7) for a harmonic motion and equation (8), the following equations can be derived:

$$s = \omega_0^2\,X/(\omega^2 - \omega_0^2) \tag{9}$$

$$s = \omega_0^2\,X/(\omega^2 - \omega_0^2) \tag{10}$$

By substituting equation (10) for (5) and with regard to equation (8), the equation of the motion for the system can be written as in the following:

$$F = [M + (K/\omega^2 - \omega_0^2)]\,X \tag{11}$$

Comparing with the second law of Newton, the effective mass of the MAMM unit cell can be calculated by equation (12):

$$M_{eff} = M + (K/\omega^2 - \omega_0^2) \tag{11}$$

Based on the following equation, the effective mass and correspondingly the effective mass density of the UC can turn to negative values, which is the origin of extraordinary characteristics of AMMs in wave attenuation.

FEM Analysis

The software Abaqus version 6.14 was used to perform FEM studies in order to understand the performance of a MAMM unit cell (UC) and also to examine, whether MAMM can be used on structures to successfully reduce their vibrations. The MAMM cells were mounted on a cantilever beam to attenuate its vibrations at its first natural frequency of 600 Hz. The supposed beam in this study is an aluminium T-shaped one with a length of 30 cm, shown schematically in **Fig. 2**. The UC modeling was performed in a way that the first natural frequency of the UC steel frame was adjusted to 600 Hz, similar to the supposed beam, by modifying its stiffness. Later, during the beam simulations, the stiffness of the frame was restored to steel stiffness of 210 GPa. Using this approach, it was planned to tailor the disk resonance in sake for attenuation of beam vibrations at its first resonance mode. Moreover, different configurations for MAMM UC were thought up and modeled, in which multiple local resonances are generated within a UC by using multiple resonators in separated membranes. The goal is to increase the operation frequency range of MAMM and find out its behavior.

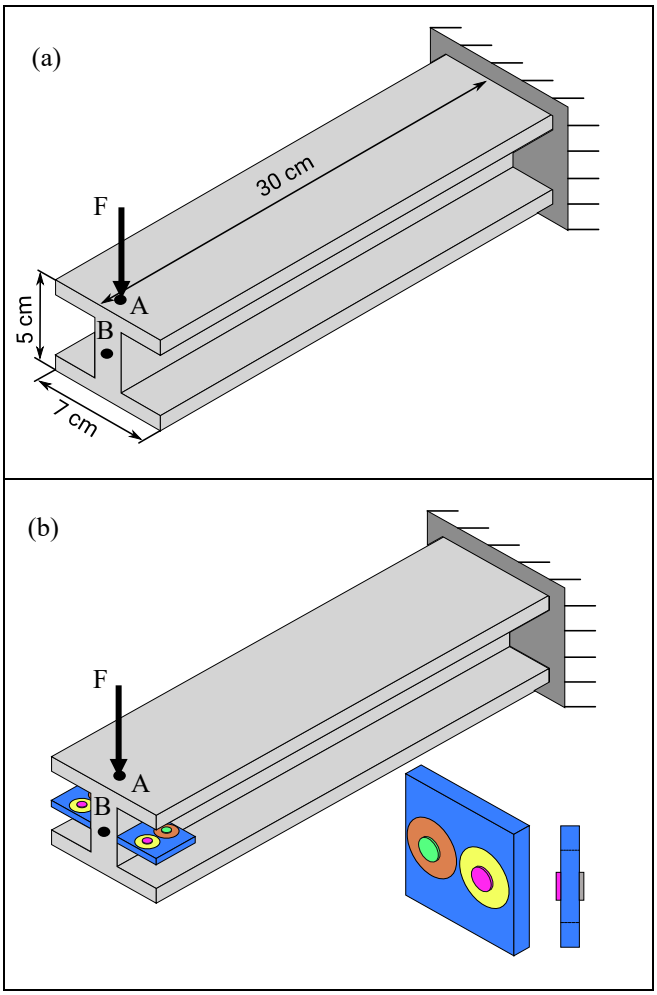

Fig. 2– (a) Schematic view of the modeled beam in this study and the applied boundary conditions to it. The force F is applied on point A and the resulted velocity level is caluclated at point B (b) Application of MAMM UCs with Config. 4 on the identical beam in (a) to attenuate its vibration

The study started with modeling a simple MAMM UC with a single resonator and membrane (Config. 1 in **Table 1**). The resonator disk is modeled as a rigid body, meaning it is not deformed in contact to the elastic membrane, which reduces the calculations by simulation. The frame is excited with a concentrated force on point A', shown in **Fig. 3**, and the consequent velocity level at point B' is calculated to monitor

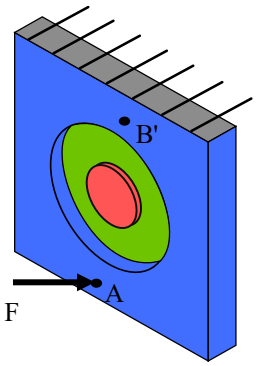

Fig. 3– Applied boundary conditions on a UC. Force F on point A' excites the frame and the velocity level is calculated accordingly on point B'

the behavior of the system. Based on this configuration, the double resonator Config. 2 was built up, in which the two resonators are concentrically placed on sides of the frame. Later, configurations 3 and 4, respectively with two and four resonators were modeled. Using different resonators and membranes in a UC facilitates the tailoring of the AMM to the desired frequencies. Based on equation (8), the local resonance frequency can be adjusted by altering the stiffness of the elastic membrane or the mass of the resonator. These two quantities can be in turn manipulated by changing the dimensions and densities of the resonators and the membranes and also through changing the elasticity modulus of the membrane. This brings a variety of possibilities to tailor the local resonances. The local resonance frequencies in the studied configurations are stated also in **Table 1**. A summary of dimensional and mechanical properties of the materials in this study is listed in **Table 2**. At the end, the improved UC, namely UC with configuration 4, was mounted on the mentioned beam (see **Fig. 2**), to examine its influence on first natural mode of the beam. For a better comprehension, the AMM-beam was compared with the same beam in absence of MAMM unit cells.

Table 1– Different studied configurations of MAMM UC; with (1) one central resonator (2) two concentric resonators on sides of the frame (3) two side-by-side resonators (4) four resonators, consisting of side-by-side resonators on each side of the frame

Config.	Schematic View	Components	Resonance Frequency [Hz]
(1)	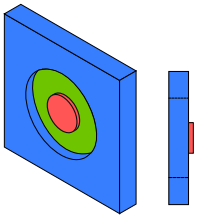	Res.1 Mem.1 Frame (C)*	577
(2)	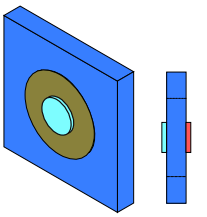	Res.1 Res.2 Mem.1 Mem.2 Frame (C)*	542, 580
(3)	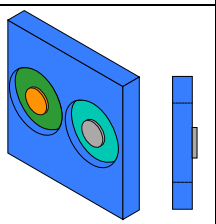	Res.3 Mem.3 Mem.4 Frame (S)**	559, 590
(4)	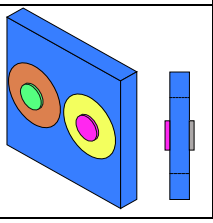	Res.3 Res.4 Mem.3 Mem.4 Frame (S)*	559, 582, 594, 607

* One central hole in the frame
** two side by side holes in the frame

Table 1– Dimensional and mechanical properties of materials

Component	Dimensions [mm]	Material	Mass Density [g/cm³]	Weight [mg]	E [GPa]	Poisson's ratio	Damping [%]
Res. 1	r = 5 t = 1	Alu	2.7	210	N/A(1)	N/A	N/A
Res. 2	r = 4 t = 1	PLA	1.5	75	N/A	N/A	N/A
Res. 3	r = 3 t = 1	Alu	2.7	76.5	N/A	N/A	N/A
Res. 4	r = 3 t = 1	-- (2)	2.48	70	N/A	N/A	N/A
Mem. 1	r = 8 t = 0.7	Silicon Rubber	1.2	168	0.09	0.47	3
Mem. 2	r = 8 t = 0.65			157			
Mem. 3	r = 6.5 t = 0.6			96			
Mem. 4	r = 6.5 t = 0.63			100			
Frame (C)	a = 30 t = 3	St.	7.85	16500	12/ 210 (3)	0.28	0.2
Frame (S)	a = 30 t = 3	St.	7.85	14900	17 /210	0.28	0.2
Beam	(4)	Alu	2.7	919	70	0.33	0.2

Res. = Resonator
Mem. = Membrane
(1) Not applied to the rigid model
(2) No real material
(3) Values respectively for UC and beam simulations
(4) in accordance with Fig. 2

The results of configurations 1 and 2 are shown in **Fig. 4**, in comparison with the base frame without any resonator. The original resonance of the frame at 600 Hz is shifted to about 627 Hz by applying configuration 1 of MAMM due to local resonance of the resonator at 577 Hz, resulting an anti-resonance effect at 600 Hz. The single resonance of the frame is this way substituted by two resonances, the shifted resonance of the frame and the local resonance of the resonator. Not only a great degree of wave attenuation is attained at the anti-resonance point, but also the velocity

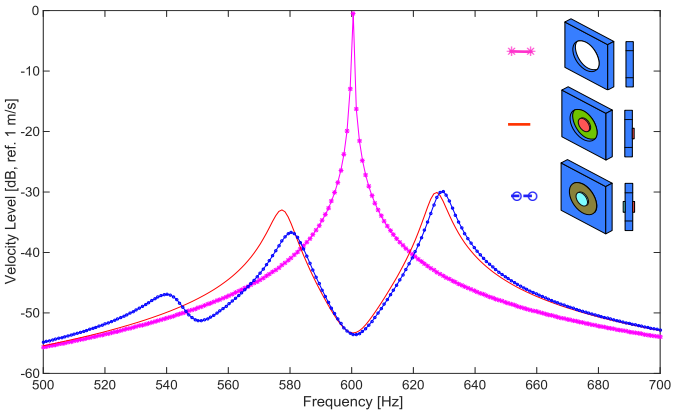

Fig. 4– The wave attenuation at point B' in the frame of a MAMM configuration, in accordance with Fig. 3, respectively in absence of resonators as well as with one and two central resonators

levels at the peak points is reduced to a great degree, meaning a lower level of vibration in the frame structure. Using configuration 2, the same effect can be brought at another frequency. The second resonator improves the system in an important point of view, as it improves the system response at lower frequencies by reducing the peak point wave level of the first resonator. This is especially important regarding the challenging insulation of waves at lower frequencies.

The response of the system by application of MAMM configurations 3 and 4 are illustrated in **Fig. 5**. The behavior of the system with configuration 3 is generally similar to configuration 2, which is expected due to equal number of local resonances by them. Using four resonator in a UC in configuration 4, leads to a greater total wave attenuation and lower levels at peak points.

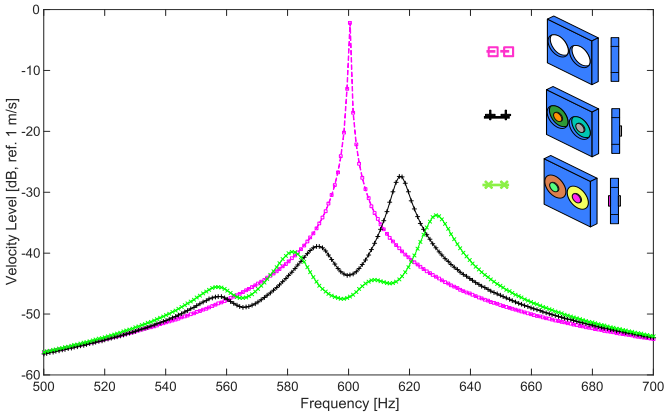

Fig. 5– Wave attenuation at point B' in the frame of a MAMM configuration in accordance with Fig. 3, respectively in absence of resonators as well as with two and four side by side resonators

In the last stage of the study, two UCs with config. 4 are mounted on the mentioned beam. The results are shown in **Fig. 6**. Similar to UC simulations, the velocity level is reduced to a great degree by using MAMM in the beam. However, the general curve of the sound velocity level against frequency seems different than of the config. 4 in **Fig. 5**, which indicates the need for deeper study and analysis of the system. The improvement of wave attenuations by multiple resonator is dependent on suitable tailoring of the local resonances.

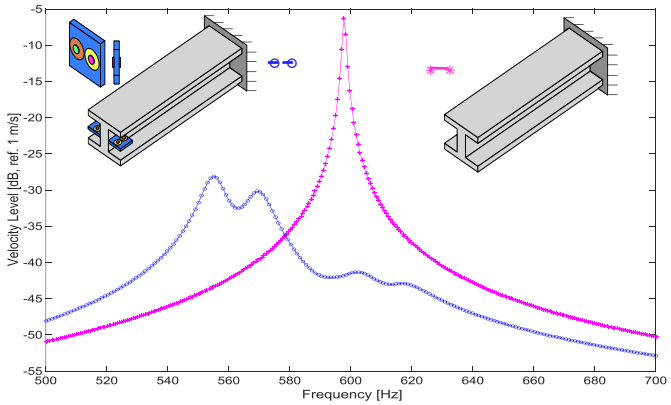

Fig. 6– Wave attenuation at point B of a cantilever beam, in accordance with Fig.2, due to application of a MAMM configuration with four resonators per UC

Conclusion

This study showed the feasibility of using membrane acoustic metamaterials on structures to attenuate their vibrations. It was shown, that the performance of MAMMs and their operation frequency range can be improved by locating multiple different local resonances within the UC. However, further deeper studies are required in order to comprehend the tailoring of AMM and the related influencing parameters to it. Also, the influence of local resonances on each other should be studied more exactly. This research focused on numerical studies, which are to be evaluated experimentally. Moreover, further studies are required to understand tailoring parameters of MAMMs and in general AMMs. On the other hand, the design and construction complexities of acoustic metamterials remains as an obstacle for their commercial and large scale production and application in the industry.

Literatur

1. Fok, L., Ambati M., Zhang X. MRS Buletin 2008; Vol. 33; issue 10; pp. 931-934.
2. Ma G., Sheng, P.; Acoustic Metamaterials: From Local Resonances to Broad Horizens. Sci. Adv. 2016; vol.2, no. 2; e1501595.
3. Nojavan A., Ring T., Langer S.C.; Vibration Attenuation in a Beam Using Acoustic Metamaterial; Conference Paper; Inter-Noise 2017; Hong Kong 2017; pp. 3173-3180.
4. Liu Z., Zhang X., Mao Y., Zhu Y., Yang Z., Chan C., Sheng P.; Locally Resonant Sonic Materials; Science 2000; Vol 29; p 1734-1736
5. Yang Z., Mei J., Yang M, Chan N.H., Sheng P.; Membrane-Type AcousticMetamaterial with Negative Dynamic Mass; Physical Review Letters 2008; Vol 101; No. 20; DOI 10.1103/phys-revlett.101.204301
6. Yang Z., Dai H. M., Chan N.H., MA G.C., Sheng P.; , Acoustic Metamaterial Panelsfor Sound Attenuation In The 50–1000 Hz Regime; Letters 2010; Vol 96; No. 4; DOI 10.1063/1.3299007
7. Fan L., Chen Zh., Zhang S. Y., Ding J.; Li X. J.; Zhang H.; An Acoustic Metamaterial Composed Of Multi-Layer Membrane-Coated Perforated Plates For Low-Frequency Sound Insulation; Applied Physics Letters 2015; Vol 101; No. 15; DOI 10.1063/1.4918374
8. Wang X., Zhao H., Luo X., Huang Zh.; Membrane-Constrained Acousticmetamaterials For Low Frequency Sound Insulation; Applied Physics Letters 2016; Vol 108; No. 4; DOI 10.1063/1.4940717